JOURNAL OF COMPUTATIONAL PHYSICS 114, 298–307 (1994)

# Algorithm for Random Close Packing of Spheres with Periodic Boundary Conditions

ALEXANDER Z. ZINCHENKO

*Institute of Mechanics, Moscow University, 119899 Moscow, Russia**

Received March 17, 1993; revised January 6, 1994

The isotropic algorithm is constructed for random close packing of equisized spheres with triply periodic boundary conditions. All previously published packing methods with periodic boundaries were *kinetics-determined*; i.e., they contained a densification rate as an arbitrary parameter. In contrast, the present algorithm is *kinetic-independent* and demonstrates an *unambiguous* convergence to the experimental results. To suppress crystallization, the main principles of our algorithm are (1) to form a contact network at an early stage and (2) retain contacts throughout the densification, as far as possible. The particles are allowed to swell by the numerical solution of the differential equations of densification. The RHS of these equations is calculated efficiently from a linear system by a combination of conjugate gradient iterations and exact sparse matrix technology. When an excessive contact occurs and one of the existing bonds should be broken to continue the densification, an efficient criterion based on multidimensional simplex geometry is used for searching the separating bond. The algorithm has a well-defined termination point resulting in a perfect contact network with the average coordination number six (for particle number $N \gg 1$) and a system of normal reactions between the spheres maintaining the structure. These forces are the counterpart of the algorithm and can be used to calculate small elastic particle deformations in a granular medium. Extensive calculations are presented for $50 \leqslant N \leqslant 400$ and demonstrate very good agreement with the experimental packing density (about 0.637) and structure. 

## 1. INTRODUCTION

Random close packing (RCP) of spheres has been extensively studied for many years [1–19] because it serves as a useful model for amorphous solid glasses and supercooled liquids. Our main interest to the problem is, however, in its relevance to calculating the effective thermal conductivity of granular media with highly conducting inclusions [20]. A quite efficient algorithm for the solution of the thermal boundary-value problem for $N$ spheres has been recently developed, with allowance for periodic boundary conditions [21]. So it seems attractive to apply this algorithm to computer simulated RCP configurations with large (up to hundreds) particle number $N$, thus providing, for the first time, a simulation test for Batchelor and O'Brien's semiempirical theory [20]. Note that any suitable computer RCP realizations should have particles in (almost) perfect contact, otherwise the conductivity calculations will be strongly affected by the gaps between the inclusions. Roughly, it follows from [20] that for the average gap $h$ the condition $\gamma^2 h/a \leqslant O(1)$ should be met, with $a$ being the particle radius and $\gamma$ being ratio of particle-to-medium conductivities. The latter condition becomes a severe limitation to particle geometry for $\gamma > 10^2$.

From the experimental view point, the RCP is a well-reproducible statistical state which is obtained by long vibration of a large container full of steel balls and extrapolating the measured quantities, e.g., the packing density (particle volume fraction) $c$ to eliminate finite-size effects [1]. Computer simulation of RCP configurations is, however, a severe problem, which has not yet obtained a satisfactory solution.

The first group of methods [3–8] use sequential addition of spheres to a randomly packed bed, but the attainable packing densities are for too low (not exceeding 0.606), compared to the experimental RCP density $0.6366 \pm 0.0005$ [1]. The algorithms for sequential placement of spheres around a central [9–11] also do not lead to the experimental RCP density, as the cluster size tends to infinity [12]. Besides, all these methods do not allow for triply periodic boundary conditions. Without the implementation of periodic boundaries, it is practically impossible to accurately attain the limit $N \to \infty$ in conductivity simulations.

It is commonly believed [13–15] that the RCP density corresponds to the singularity in the equation of state for a hard-sphere fluid along the supercooled metastable branch and there have been simulations exploiting this idea [16–17]. In particular, Woodcock [17] carried out 500-sphere molecular dynamics simulation, allowing particles to swell gradually. As the free volume approaches

* Present address: Department of Chemical Engineering, University of Colorado, Boulder, CO 80309-0424.

0021-9991/94 $6.00

zero, the time required to affect further increase in particle volume fraction $c$ grows exponentially [17], and the limiting packing density was obtained by extrapolating to infinite time. Despite the attractive agreement with the experimental RCP density [1], this extrapolation seems unsuitable for preparing RCP configurations with a perfect contact structure. More discouragingly, any molecular dynamics or Monte-Carlo-like densification procedures are *kinetics-determined*; i.e., they contain the densification rate as an arbitrary parameter. For $N \leqslant O(100)$ (the range tractable in conductivity simulations), when the true metastability is not yet formed, the final packing density is strongly sensitive to densification rate [18] and practically any degree of crystallization can be obtained for sufficiently slow compression.

The more recent algorithms [12, 19] generate high density irregular packing of spheres from a random distribution of points. Eeach sphere has two diameters, the inner $d_{\text{in}}$ (which is the minimum center-to-center distance between the spheres) and the outer one $d_{\text{out}}$ (which corresponds initially to nominal packing density $c = 1$). In each iteration the closest two spheres are separated along the line of centers until their center-to-center distance equals $d_{\text{out}}$ and then $d$ shrinks slightly. So the two diameters approach each other and the process is terminated once $d_{\text{in}} \geqslant d_{\text{out}}$. The main difference of [19] from [12] is the variable rate of contracting the outer diameter; that depends on some arbitrary parameter $k$. Significantly, in the final packing the particles are not touching and the contact network is formed only in the limit $k \to 0$, for fixed $N$. The algorithm [12, 19] is very fast (especially in the code [22]) compared to usual hard-sphere fluid compression (see above) and excellent agreement with the experiment was reported in [12] for 3000 simulated particles. This success is, however, misleading. The particles in [12] were not in perfect contact (unlike experimental structures); the average coordination number (defined via surface neighboring within $10^{-2}a$) was about 5.4, instead of being slightly above the true value 6. More discouragingly, it was shown in [19] for the same order of particle number ($N = 1000$) that a much slower contraction of the outer diameter results in appreciably higher packing density, up to 0.649–0.650 (see also [23]). Our calculations using the algorithm [19] suggests even a higher packing density, at least 0.666 in the limit $k \to 0$, $N \to \infty$ (see Section 3). From our viewpoint, this deviation from the experiment is a consequence of some crystallization in the algorithm [19] for $k \ll 1$ (the latter becomes more evident in the force-biased algorithm [23], a further development of the method [19]). It appears (see Section 3) that "rough" packings prepared by method [19] with "not too small" values of $k$ can be considered as quite random (that is the reason for the success [12]), but they are not close packings by definition.

So, a strong motivation exists to work out a quite new, *kinetics-independent* (i.e., containing no densification rate) algorithm with *unambiguous*, single-valued convergence to the experimental results on RCP. Note that the gaps between the particles at the *intermediate* stage of densification are the very reason for partial crystallization in a slowly compressed hard-sphere fluid. Indeed, in the "solid region" $c > 0.55$ molecular dynamics and Metropolis' scheme [24] of the Monte-Carlo method act as crystallizing mechanisms. These mechanisms would be prohibited if the particles had already formed a contact network. Partial crystallization in the algorithm [19] has a similar (but more subtle) reason, since at the intermediate stage there are also considerable gaps between the spheres of the inner diameter, whatever small $k$ is. So, to suppress crystallization, the main principles of our algorithm are (1) to form a touching network at an early stage and (2) to retain contacts throughout the densification, as far as possible. This isotropic algorithm resembles the physical situation when $N \gg 1$ smooth spheres having been poured into a large vessel slide along each other until the RCP state is formed (from this viewpoint, the only role of small vibration is to eliminate friction temporarily). The algorithm allows particles to swell while keeping the contacts by numerical solution of the *differential equations of densification* (derived in the present work), resulting in *collective* displacement of spheres at each integration step. The RHSs of the equations are calculated from the linear system for $3N$ unknowns using some efficient combination of conjugate gradient iterations and exact sparse matrix technology. Roughly, the densification consists of two stages: (1) the initial stage, when a full structure of about $3N$ contacts is formed and (2) the main stage, when excessive contacts occur, and each time one of the existing bonds should be broken to continue the densification. (The description of the main stage is given first, to provide a better view of the whole method). The efficient criterion for searching separating bonds is the crucial part of the algorithm and turns out to be connected to the geometry of a simplex in multidimensional space. The algorithm has a well-defined termination point, when no bond can be separated after an excessive contact has occurred. The algorithm is purely geometrical, but the final state has a clear physical sense. Namely, a non-zero system of normal contact reactions exists which maintains the structure (against the confining pressure, if applied) and prohibits further densification. The calculation of these reactions happens to be a part of the algorithm. The latter is of physical significance for future studies since it allows us to calculate small particle deformations on the microscale quite rigorously using Hertz theory [25]. These deformations are known to affect drastically the conductivity of granular media [20].

The numerical results obtained for $50 \leqslant N \leqslant 400$ are discussed in Section 3. All the calculations have been performed on PC AT ACRO 386 c, with Weitek 3167 as a floating point accelerator and about 3 Mbytes of useful memory.

Albeit our algorithm is mathematically more complicated than the other packing codes, it is, to the best of our knowledge, the only one that demonstrates a *single-valued* convergence to the experimental RCP density (very close to 0.637) and, at the same time, produces a perfect contact structure (with the average coordination number 6). The radial distribution function is also in very good agreement with the experiment. The concept of bonded (contacting) particles has a true sense in our approach, unlike conditional neighboring in [12, 19] which depends on an arbitrary tolerance $\delta$. The actual gaps between bonded particles in our algorithm that depend on the integration step can be made exceedingly small in practice (see Section 3).

The intermediate stage of our densification procedure may not correspond exactly to any physical situation. In a different quasi-static approach [26] the system is densified, being subjected to cyclic shear, with elastic and frictional forces taken into account, which is a more realistic model. However, for three dimensions only preliminary results were reported, with 90 spheres in a periodic box densified to $c = 0.58$, so it is yet impossible to compare this new approach with the present method.

## 2. METHOD

### 2.1. *Main Stage of the Densification*

Consider an infinite set of equisized non-overlapping spheres of radius $a$. The particle system is obtained from the basic random configuration of spheres $S_1, ..., S_N$ centered at $\mathbf{x}_1, \mathbf{x}_2, ..., \mathbf{x}_N \in V$ by the triply periodic continuation into all space with the periods 1, 1, 1 ($V = [0, 1) \times [0, 1) \times [0, 1)$ being the unit cubic cell). Let the system of spheres initially form a touching network with $3N-3$ independent contacts and each particle having at least three neighbors. Let $\mathbf{k}_{ij}$ be the integer vector so that $\mathbf{x}_j + \mathbf{k}_{ij}$ is the center of the periodically replicated $S_j$ that is nearest to $S_i$ and

$$\mathbf{x}_{ij} = \mathbf{x}_j + \mathbf{k}_{ij} - \mathbf{x}_i \tag{1}$$

is the corresponding center-to-center minimal vector. The following geometric relations then hold for the contact pairs $(i_k, j_k)$ $(1 \leqslant i_k < j_k \leqslant N)$:

$$\mathbf{x}^2_{i_k, j_k} = (2a)^2 \qquad \text{for} \quad k = 1, 2, ..., 3N-3. \tag{2}$$

The constraints (2) form $3N-3$ non-linear equations for $3N$ unknown coordinates $x_i, y_i, z_i$ and are invariant when an arbitrary vector constant is added to all $\mathbf{x}_i$. So, up to an insignificant translation of the whole particle configuration, the system (2), in general, may have only a finite number of isolated solutions (that presumably differ from each other only by the particle permutation) and, without any loss of generality, one can consider the sphere positions $\mathbf{x}_i$ satisfying (2) as unique functions of the particle radius $a$. Introducing the "velocities"

$$\frac{d\mathbf{x}_i}{da} = \mathbf{V}_i \tag{3}$$

and differentiating (1) with respect to $a$ we have

$$\mathbf{x}_{i_k, j_k} \cdot (\mathbf{V}_{j_k} - \mathbf{V}_{i_k}) = 4a \qquad \text{for} \quad k = 1, 2, ..., 3N-3. \tag{4}$$

It is convenient to exclude an insignificant shift of the whole system by setting

$$\sum_{i=1}^{N} \mathbf{V}_i = 0. \tag{5}$$

The linear equations (4)–(5), in general, define the "velocities" $\mathbf{V}_i$ as unique functions of $a$ and $\mathbf{x}_1, ..., \mathbf{x}_N$. So, (3) can be considered as a system of differential equations for $\mathbf{x}_i(a)$ and integrated numerically, *which allows particles to swell while keeping all the existing contacts.* However, during the densification a new contact $k = 3N-2$ may occur. At that moment the system (4)–(5) with the new contact equation for $k = 3N-2$ becomes overdetermined, and one of the existing bonds with $k = k^* \leqslant 3N-3$ has to be broken to continue the densification. Obviously, the value of $k^*$ cannot be arbitrary because at this moment the solution $\mathbf{V}_i$ of the system

$$\mathbf{x}_{i_k, j_k} \cdot (\mathbf{V}_{j_k} - \mathbf{V}_{i_k}) = 4a \qquad \text{for} \quad k = 1, 2, ..., 3N-2, \; k \neq k^*, \tag{6}$$

should necessarily satisfy the separation condition

$$\mathbf{x}_{i_k, j_k} \cdot (\mathbf{V}_{j_k} - \mathbf{V}_{i_k}) > 4a \qquad \text{for} \quad k = k^*. \tag{7}$$

The problem of unique and efficient choice of $k^*$ is discussed later (Section 2.2). Once $k^*$ has been specified and excluded from the list of contact bonds, we continue densification by the numerical integration of (3), with the "velocities" $\mathbf{V}_i$ calculated at any moment from (4)–(5) until a new contact occurs and so on. Eventually it turns out, after some new contact formation, that no $k^*$ can satisfy the separation condition (7). It will be shown later that this well-defined termination point corresponds to random close packing (provided that the initial state is random) and that the physical normal reactions between the spheres exist to maintain the structure. Note that this algorithm is essentially "static"; i.e., it contains no densification rate $da/dt$. The principal idea of this algorithm is simple, but the robust and efficient computer realization meets some difficulties and is discussed below.

2.2. *An Efficient Separation Criterion*

The most direct way to find $k^*$ would be multiple solutions of the systems (6) for all $k^* = 1, 2, \ldots$ until (7) is satisfied. However, near RCP only a small portion of bonds can be separated and one would have to check almost all the values $k^* \in [1, 3N-3]$, which is extremely inefficient, especially for large $N$ when the analysis of contacts is the most time-consuming part. Besides, the choice of the first value of $k^*$ satisfying (7) does not generally meet the stability condition (see below). Fortunately, a quite efficient algorithm for selecting all the values of $k^*$ satisfying (7) can be proposed based on multidimensional simplex geometry.

Consider a more general problem. Let

$$\begin{aligned} a_{11}x_1 + \cdots + a_{1m}x_m - b_1 &= 0, \\ &\cdots \\ a_{k1}x_1 + \cdots + a_{km}x_m - b_k &= 0, \\ &\cdots \\ a_{m+1,1}x_1 + \cdots + a_{m+1,m}x_m - b_{m+1} &= 0 \end{aligned} \tag{8}$$

be a general overdetermined system of $m+1$ equations for $m$ unknowns $x_1, \ldots, x_m$. Let $\mathbf{P}^{(k)} = (x_1^{(k)}, \ldots, x_m^{(k)})$ be the solution of the system (8) without the $k$th equation and let

$$\delta_k = a_{k1}x_1^{(k)} + \cdots + a_{km}x_m^{(k)} - b_k \tag{9}$$

be the residual due to substituting $\mathbf{P}^{(k)}$ into the deleted equation. Let $\mathbf{x}^*$ be the minimizing point for the function

$$F(\mathbf{x}) = \sum_{i=1}^{m+1} (a_{i1}x_1 + \cdots + a_{im}x_m - b_i)^2 \tag{10}$$

and let

$$\varepsilon_k = a_{k1}x_1^* + \cdots + a_{km}x_m^* - b_k \tag{11}$$

be the residual due to substituting $\mathbf{x}^*$ into the $k$th equation (8).

LEMMA (*For the proof, see the Appendix*).

$$\delta_1\varepsilon_1 = \delta_2\varepsilon_2 = \cdots = \delta_{m+1}\varepsilon_{m+1} > 0. \tag{12}$$

According to (12), an efficient algorithm for searching the values of $k$ with $\delta_k > 0$ requires just calculating the extremal point $\mathbf{x}^*$ by a *single* solution of the linear system $\partial F/\partial x_i = 0$ and then checking $\varepsilon_k > 0$.

In the case of the RCP problem,

$$F = \sum_k [\mathbf{x}_{ik,jk} \cdot (\mathbf{V}_{jk} - \mathbf{V}_{ik}) - 4a]^2 \tag{13}$$

and the extremal point $(\mathbf{V}_1^*, \ldots, \mathbf{V}_N^*)$ satisfies $\partial F/\partial \mathbf{V}_i = 0$, i.e.,

$$\sum_{j \in \mathscr{A}_i} [4a - \mathbf{x}_{ij} \cdot (\mathbf{V}_j^* - \mathbf{V}_i^*)]\, \mathbf{x}_{ij} = 0 \qquad \text{for} \quad i = 1, \ldots, N, \tag{14}$$

where $\mathscr{A}_i$ is the whole set of neighbors of particle $i$, with allowance for periodicity. The choice of the separating bond is still not unique since there may be many contact pairs $(i,j)$ with $\mathbf{x}_{ij} \cdot (\mathbf{V}_j^* - \mathbf{V}_i^*) - 4a > 0$. Two strategies were tested: (1) random equiprobable selection of the separating bond among those with $\mathbf{x}_{ij} \cdot (\mathbf{V}_j^* - \mathbf{V}_i^*) - 4a > 0$ and (2) the selection of the bond with maximum $\mathbf{x}_{ij} \cdot (\mathbf{V}_j^* - \mathbf{V}_i^*) - 4a$ to be broken. It was found that the choice (1) leads to the instability of the algorithm (for $N \gg 1$), whereas the strategy (2) was always quite successful and was then used exclusively in the calculations. Note that, according to (12), the maximum of $\mathbf{x}_{ij} \cdot (\mathbf{V}_j^* - \mathbf{V}_i^*) - 4a$ corresponds to the choice of the bond which is separated with the *least* possible "velocity" $\mathbf{x}_{ij} \cdot (\mathbf{V}_j - \mathbf{V}_i) - 4a$. The latter matches quite naturally our strategy of keeping contacts during the densification.

It is particularly useful to interpret (14) physically by writing it in the form

$$\sum_{j \in \mathscr{A}_i} N_{ij}\mathbf{x}_{ij} = 0, \tag{15}$$

where

$$N_{ij} = -\lambda[\mathbf{x}_{ij} \cdot (\mathbf{V}_j^* - \mathbf{V}_i^*) - 4a] \tag{16}$$

and $\lambda > 0$ is an arbitrary constant. According to (15), at the moment of a new contact formation with $3N-2$ independent bonds there is a non-trivial system (which is unique, up to a factor) of normal contact forces maintaining the structure. Obviously, our strategy is simply to choose the bond with the "most negative" $N_{ij}$ to be broken. At RCP all $N_{ij}$ are non-negative and can be interpreted as real normal reactions maintaining the particles and prohibiting further densification. The constant $\lambda$ can be connected to the average pressure in the bed.

Note that during the densification and at RCP there is a very small, but usually non-zero portion of particles having only three neighbors each. The degenerate case of the bond $(i,j)$ with either particle $i$ or $j$ having three neighbors corresponds to $N_{ij} = 0$ and these bonds are explicitly prohibited to break in the algorithm.

2.3. *Efficient Scheme for Determining the "Velocities"* $\mathbf{V}_i$

Instead of solving the system (4), it is much more convenient numerically to replace it by the problem of minimiz-

ing the function (13) (with min $F=0$) and reduce (4) to a new system

$$-\sum_{j\in\mathscr{A}_i}[\mathbf{x}_{ij}\cdot(\mathbf{V}_j-\mathbf{V}_i)]\,\mathbf{x}_{ij}=-4a\sum_{j\in\mathscr{A}_i}\mathbf{x}_{ij}, \qquad (17)$$

the only difference from (14) being the number of contact bonds ($3N-3$ instead of $3N-2$). Fast numerical solution of (14) and (17) should use effectively the sparsity of these systems. Usual iterative procedures turned out to be too inefficient for systematic use due to great ill-conditioning at $N\gg 1$. Even the most successful, conjugate gradient method (CGM) (in the classical form [27]) required about $3N$ iterations (or even much more, due to round-off errors) for an acceptable accuracy at the moments of a new contact formation, when the bond structure changes and no good initial approximation can be guessed. The most efficient strategy for the solution of (17) was found to be a combination of the two methods: (1) direct solution by sparse matrix technology [28] and (2) iterative solution by preconditioned CGM (e.g., cf. [27]) using the factorization prepared by method (1) at some previous integration step.

In the method (1) we first set $\mathbf{V}_l=0$ for the particle $l$ with maximum coordination number, thus making the LHS of (17) a self-adjoint positive definite operator in the space of $\mathbf{V}_1,\ldots,\mathbf{V}_{l-1},\mathbf{V}_{l+1},\ldots,\mathbf{V}_N$. Then the LHS matrix is factorized into Cholesky product $S^{\mathrm{T}}S$, where $S$ is an upper triangle matrix and each element of $S$ being a $3\times 3$ block. The particles are reordered beforehand by Tinney and Walker's minimum degree algorithm [28], to reduce considerably the number of non-zero blocks in $S$. The solution of the factorized system (17) can be then shifted by a vector constant to satisfy (5). For maximum efficiency, the sparse matrix technology is built in the algorithm (in particular, taking full advantage of the block structure of $S$), instead of using library sparse matrix packages. Due to block structure of $S$, the floating-point arithmetics in factorizing (17) (or (14), see below) is the most time-consuming part and the one to be optimized. As for minimum degree algorithm, a much simpler implementation than in [28] suffices and takes only about 5% of the total factorization time (for $50\leqslant N\leqslant 400$).

In the method (2) the system (17) written in the matrix form $A\mathbf{V}=\mathbf{b}$ is replaced by

$$(S^{\mathrm{T}})^{-1}AS^{-1}\mathbf{U}=(S^{\mathrm{T}})^{-1}\mathbf{b}, \qquad (18)$$

$$\mathbf{U}=S\mathbf{V}, \qquad (19)$$

where $S$ is the Cholesky factor obtained by method (1) at some previous and close integration step so that $A\approx S^{\mathrm{T}}S$. The self-adjoint positive-definite system (18) is solved iteratively by CGM, the convergence being generally very fast since $(S^{\mathrm{T}})^{-1}AS^{-1}$ is close to identity matrix. The system (17) is always solved exactly by factorization at the initial moment and at the moments of a new contact formation as soon as the bond $k=k^*$ is excluded from the list of contact pairs. It is usually unnecessary to calculate additional factorizations and the solution of (18) between the contacts takes generally one, at most two iterations, if the initial approximation to $\mathbf{V}_i$ is chosen as described in Section 2.4. The system (14) for determining $k^*$ is always solved by method (1).

Table I presents the average computer run-times $T_f$ (seconds) for factorizing (14) or (17) and $T_{it}$ (seconds) for the iterative solution of (17) (one iteration) on PC AT ACRO 386 c/Weitek 3167 for typical values of $N$. These results suggest that $T_f$ scales like $N^{5/2}$ and $T_{it}$ like $N^{3/2}$. For this reason, the twofold factorizations at the moments of a new contact formation were the most time-consuming in our calculations for the largest values of $N$.

### 2.4. *Initial Stage of Densification*

A somewhat different technique is used to prepare the initial configuration of particles forming a touching network with $3N-3$ independent contacts (each particle having at least three neighbors) so that the system (4)–(5) is uniquely soluble (this state is subsequently referred to as a "full contact structure"). We start from an equilibrium configuration of non-touching spheres prepared by the usual Metropolis' method [24] at some particle volume fraction $c_0$ in the "fluid region" $c_0<0.49$ [29] (to ensure complete disorder) and allow the particles to swell until the first contact occurs. After that the system (3) is integrated numerically, with new contacts joining one at a time. The "velocities" $\mathbf{V}_i$ satisfy (4), with $3N-3$ replaced by a current number of contacts, and are calculated iteratively from (17) by the usual CGM (without preconditioning). The difference from the case of a full contact structure is that (5), (17) now form an *underdetermined* system and the solution $\mathbf{V}_i$ depends on the initial approximation $\mathbf{V}_i^{(0)}$. The specific feature of CGM is to select the solution of (17) with minimum $\|\mathbf{V}-\mathbf{V}^{(0)}\|$ (in the Euclidean norm). To ensure the smoothness of the process (or the least possible jump of the "velocities" $\mathbf{V}_i$ at the moments of a new contact formation) and to promote con-

**TABLE I**

Typical Computer Run-Times $T_f$ (s) of Factorizing the System (14) or (17) by Sparse Matrix Technology and $T_{it}$ (s) of the Iterative Solution of System (17) by Preconditioned Conjugate Gradient Method (One Iteration) on a PC AT ACRO 386 c/Weitek 3167, for Different Values of Particle Number $N$

| $N$ | 50 | 100 | 200 | 400 |
|---|---|---|---|---|
| $T_f$ | 0.3 | 1.4 | 6.7 | 38 |
| $T_{it}$ | 0.07 | 0.16 | 0.4 | 1.2 |

*Note.* For two iterations $T_{it}$ should be increased by a factor of 1.5.

vergence, a linear extrapolation of the converged vectors $\mathbf{V}_i$ from the two previous integration steps is taken as $\mathbf{V}_i^{(0)}$ (for the step immediately after the contact only the last values of $\mathbf{V}_i$ are used as the initial approximation). A different opportunity of generating random normally distributed vectors $\mathbf{V}_i^{(0)}$ was also tested, the convergence being much slower. It was verified that the two strategies of choosing $\mathbf{V}_i^{(0)}$ at the initial stage do not lead to any noticeable differences in the final RCP density and structure.

Even when the total number of contact pairs is still less than $3N-2$, the system (4)–(5) is observed sometimes not to have a solution (the function (13) stabilizes, up to the machine precision, to a non-zero minimum in the course of iterations). Obviously, this corresponds to the case of $N_1$ ($<N$) particles forming a full contact structure (usually $N_1 \approx N$). In this case the strategy of Section 2.2 is applied, i.e., to delete the bond with maximum $\mathbf{x}_{ij} \cdot (\mathbf{V}_j - \mathbf{V}_i) - 4a$ and solve (17) once more. So the process is continued successfully until a full contact structure including all the $N$ particles is formed. After that the sparse matrix technology is used up to RCP (as described in Section 2.3) and appears to be, on the average, up to three to five times faster (for $50 \leqslant N \leqslant 400$) than the simple iterative solution of (14) and (17) by CGM.

The most complicated phenomenon associated with the algorithm is the presence of the "singular point" in the densification process. When the total number of bonds is close to $3N-3$, a very narrow interval of the values of $a$ with high "velocities" $\mathbf{V}_i$ (and very poor convergence of CGM iterations) is frequently observed, especially for $N \gg 1$ and small $c_0$. This makes the integration step extremely small (see Section 2.5) to keep particles in almost perfect contact (e.g., for $N=400$ the stagnation for several days of computation was observed, the integration step $\Delta a$ decreasing temporarily to $10^{-12}$). The standstill in densification is, however, accompanied by noticeable tangential displacement of particles and the formation of new contacts. The nature of the "singular point" is not clearly understood. Anyway, the presence of this point appears to produce no crystallizing effect since the runs with and without a pronounced "singular point" led to essentially the same final packing density. Nor is the "singular point" of universal character, for its location is quite random. Fortunately, for finite $N \leqslant 400$, used in the calculations, the time required to pass the "singularity" was generally (but not always) small, compared to the total computation time. So, no special measures were attempted to promote the process at this point.

To ensure randomness of the final state, it seems best to obtain a full contact structure as early as possible by choosing low values of $c_0$. However, the variation of $c_0$ in the "fluid region" $c_0 < 0.49$ appears to produce no noticeable effect on the final RCP density and structure (see Section 3). So it is reasonable to set $c_0$ close to 0.49, thus reducing the computational cost of the initial densification stage. Note that in our calculations the formation of a full contact structure and the "singular point" were generally observed for particle volume fractions, 0.52–0.58.

### 2.5. *Additional Details of the Algorithm*

The only acceptable integration method for (3) was found to be the simplest first-order Euler scheme,

$$\mathbf{x}_i(a+\Delta a) = \mathbf{x}_i(a) + \mathbf{V}_i\,\Delta a, \tag{20}$$

since it *never* produces overlaps of bonded particles, provided that the "velocities" $\mathbf{V}_i$ are sufficiently accurate. Indeed, for particles $i$ and $j$,

$$\begin{aligned}(\mathbf{x}_{ij} + \mathbf{V}_{ij}\,\Delta a)^2 - [2(a+\Delta a)]^2 \\ = \mathbf{x}_{ij}^2 - (2a)^2 + 2(\mathbf{x}_{ij}\cdot\mathbf{V}_{ij} - 4a)\,\Delta a \\ + (\mathbf{V}_{ij}^2 - 4)(\Delta a)^2.\end{aligned} \tag{21}$$

If the relative "velocity" $\mathbf{V}_{ij} = \mathbf{V}_j - \mathbf{V}_i$ satisfies (4) exactly, then $|\mathbf{x}_{ij}|\,|\mathbf{V}_{ij}| \geqslant 4a$ and (21) imply that

$$\begin{aligned}(\mathbf{x}_{ij} + \mathbf{V}_{ij}\,\Delta a)^2 - [2(a+\Delta a)]^2 \\ \geqslant [\mathbf{x}_{ij}^2 - (2a)^2][1 - 4(\Delta a)^2/\mathbf{x}_{ij}^2].\end{aligned} \tag{22}$$

Hence, the LHS of (21) is non-negative if $\mathbf{x}_{ij}^2 \geqslant (2a)^2$ and if the coarse condition $\Delta a \leqslant a$ is met.

The vectors $\mathbf{V}_{ij}$ are generally very large (particularly at the "singular point") and an undesirable cumulative effect of the last term in (21) is to produce gaps between bonded particles during the bond lifetimes. It was found best to choose the integration step automatically as

$$\Delta a = \eta[\max_k |\mathbf{V}_{ik,jk}^2 - 4| + 4]^{-1/2}, \tag{23}$$

the parameter $\eta = \text{const} > 0$ being determined experimentally to retain gaps between bonded particles within a very small tolerance (see Section 3).

The search for new contacts between unbonded particles is optimized by using a chaining mesh and a linked-list structure, a usually efficient technique in molecular dynamics and granular media simulations [27, 30]. In the present case we divide the unit cell $V$ into $M^3$ equal cubic sub-cells,

$$M = [(2a + 2\Delta a + 2 \max_{1 \leqslant i \leqslant N} |\mathbf{V}_i|\,\Delta a)^{-1}], \tag{24}$$

with $[\cdots]$ being the greatest integer function and $\Delta a$ determined from (23). Obviously, the search of particles $j$ intersecting a given particle $i$ ($i<j$) in the interval $(a, a+\Delta a)$

can be restricted to 27 sub-cells surrounding $\mathbf{x}_i$, and the true integration step $\Delta a'$ to the new contact moment is found as the *exact* minimum solution (if one exists) of the equations for $\Delta a'$,

$$|\mathbf{x}_{ij} + \mathbf{V}_{ij}\,\Delta a'|^2 = 4(a + \Delta a')^2, \tag{25}$$

in the interval $(0, \Delta a)$, which is one more advantage of the simple scheme (20).

The accuracy of the iterative solution of (4) is determined experimentally to produce, on the average, the same effect on the gaps between bonded particles as the last term in (21) and, besides, to ensure non-overlapping of these particles after the integration step (23). If the step is reduced to $\Delta a'$ due to a new contact formation, then additional iterations (and recalculation of $\Delta a'$) are sometimes necessary to retain bonded particle non-overlapping after the step $\Delta a'$.

All the calculations are performed in double precision. The length of the optimized code is about 1500 FORTRAN-77 lines. The memory requirement for $N \gg 1$ is approximately $N^2 + 125N^{3/2} + 970N$ bytes.

## 3. NUMERICAL RESULTS

Extensive calculations have been performed using our algorithm for different values of $\eta$, particle number $N$, and the initial particle volume fraction $c_0$ (see Table II). The calculations are divided into 10 groups, the difference between the runs within a group being in the initial random equilibrium configuration. Some quantities of interest for the final RCP state include the packing density $c$, the average gap $\varepsilon$ (relative to particle radius) between bonded spheres and the fraction $p_3$ of particle having only three neighbors each. The angular brackets denote averaging over the corresponding group of runs. Table II demonstrates that bonded particles are in almost perfect contact, provided that the value of $\eta$ and, hence, the integration step are small.

**TABLE II**

The Parameters of RCP Realizations

| Run No. | $N$ | $c_0$ | $\eta$ | $f$ | $\langle f^* \rangle$ | $\langle \varepsilon \rangle$ | $\langle p_3 \rangle$ | $\langle c \rangle$ |
|---|---|---|---|---|---|---|---|---|
| 1–8 | 50 | 0.45 | $3\times10^{-4}$ | 5.920 | 5.940 | $1.8\times10^{-4}$ | 0.020 | 0.628 |
| 9–16 | 50 | 0.35 | $3\times10^{-4}$ | 5.920 | 5.970 | $1.9\times10^{-4}$ | 0.025 | 0.620 |
| 17–24 | 50 | 0.25 | $3\times10^{-4}$ | 5.920 | 5.985 | $1.8\times10^{-4}$ | 0.023 | 0.628 |
| 25–32 | 50 | 0.25 | $6\times10^{-5}$ | 5.920 | 5.930 | $3.8\times10^{-5}$ | 0.023 | 0.623 |
| 33–39 | 100 | 0.25 | $6\times10^{-5}$ | 5.960 | 5.980 | $3.7\times10^{-5}$ | 0.019 | 0.631 |
| 40–42 | 100 | 0.25 | $2\times10^{-5}$ | 5.960 | 5.973 | $1.2\times10^{-5}$ | 0.020 | 0.629 |
| 43–45 | 100 | 0.1 | $7\times10^{-6}$ | 5.960 | 5.967 | $6.1\times10^{-6}$ | 0.013 | 0.629 |
| 46–50 | 200 | 0.45 | $2\times10^{-5}$ | 5.980 | 5.996 | $1.5\times10^{-5}$ | 0.012 | 0.633 |
| 51 | 400 | 0.45 | $2\times10^{-5}$ | 5.990 | 6.020 | $1.6\times10^{-5}$ | 0.013 | 0.637 |
| 52 | 400 | 0.49 | $7\times10^{-6}$ | 5.990 | 6.015 | $5.9\times10^{-6}$ | 0.015 | 0.636 |

*Note.* For details, see the text.

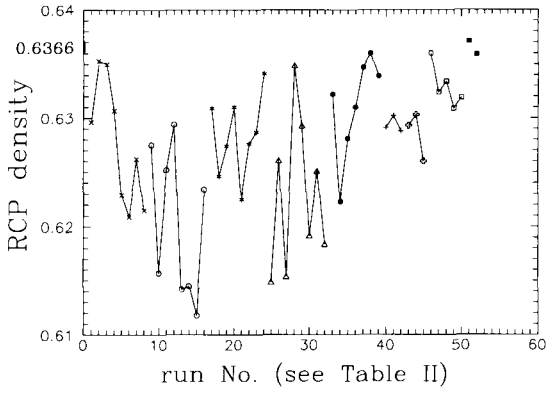


**FIG. 1.** The density of random close-packed configurations prepared by the present algorithm. The points in each group of runs with the same $N$, $c_0$, $\eta$ (see Table II) are connected.

It should be noted that this order of magnitude of $\varepsilon$ is kept throughout the whole densification. The value of $f = 6 - 4/N$ represents the nominal coordination number, i.e., the average number of bonds per particle in the RCP state. For comparison, it is also helpful to define, for each RCP configuration, $\varepsilon_{\max} a$ as the maximum gap between bonded particles and the "actual" coordination number $f^*$ as the average number of *all* near-neighbors of a particle lying within the surface-to-surface distance $\varepsilon_{\max} a$ from it. It is seen from Table II that for $\eta \ll 1$ the difference between $f$ and $f^*$ is negligibly small. So, contacting and non-contacting pairs can be truly distinguished in the limit $\eta \to 0$.

Figure 1 presents the packing density $c$ for all the calculated RCP configurations, the dispersion of the results for $N \gg 1$ being very small. The change of $c_0$ in the "fluid region" $c_0 < 0.49$ appears to produce no appreciable effect on $c$. The packing density, on the average, is an increasing function of $N$ and is definitely convergent in the limit $N \to \infty$, $\eta \to 0$ to a value about the experimental result $0.6366 \pm 0.0005$ [1]. Of course, this comparison assumes that gravitational packings can be considered as essentially isotropic and simulated using triply periodic boundary conditions. It is generally supposed (but not proved) that far from the boundaries the experimental packings contain no particles having only three neighbors. However, our algorithm does usually produce a non-zero portion $p_3$ of such spheres (as well as packing codes with sequential addition of

**TABLE III**

The Average Portion $\langle p_k \rangle$ of Particles Having $k$ Nominal Neighbors for $N = 200$ (Averaged over Runs 46–50 of Table II) and for $N = 400$ (Runs 51–52, Averaged)

| | $\langle p_4 \rangle$ | $\langle p_5 \rangle$ | $\langle p_6 \rangle$ | $\langle p_7 \rangle$ | $\langle p_8 \rangle$ |
|---|---|---|---|---|---|
| $N = 200$ | 0.108 | 0.248 | 0.301 | 0.210 | 0.096 |
| $N = 400$ | 0.114 | 0.253 | 0.280 | 0.196 | 0.119 |

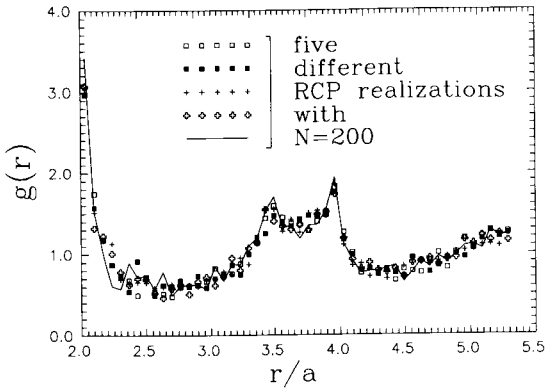


FIG. 2. Radial distribution function $g(r)$ ($r$ is the center-to-center distance) for five random close-packed configurations with $N=200$ (runs 46–50 of Table II).

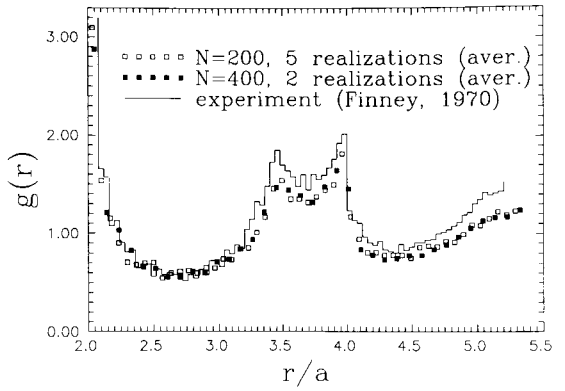


FIG. 3. The comparison of simulated radial distribution functions $g(r)$ for $N=200$ (averaged over runs 46–50 of Table II) and $N=400$ (runs 51–52, averaged) with the experimental one [2] for 7994 steel balls.

particles [4, 8]). Anyway, Table II demonstrates that the value of $\langle p_3 \rangle$ is very small, if not vanishing in the limit $N \to \infty$.

Table III presents the average portion $\langle p_k \rangle$ of particles having $k$ nominal neighbors for $4 \leqslant k \leqslant 8$. The averaged results for several runs with $N=200$ and $N=400$ are in good agreement. The statistical convergence of $\langle p_k \rangle$ for $k \geqslant 9$ is poor and these values are omitted. In contrast to the algorithms with the sequential addition of spheres (see Section 1), our packing method produces a quite different contact distribution, much closer to the experimental one (cf. our Table III and Fig. 7 of [8]), albeit the difficulty of measuring $\langle p_k \rangle$ hampers the exact comparison.

The similarity of simulated and experimental packings is further confirmed by the comparison of radial distribution functions $g(r)$. Figure 2 displays $g(r)$ for five different RCP configurations with $N=200$ (runs 46–50) indicating small dispersion of the results for $N \geqslant 200$. Figure 3 presents the averaged functions $g(r)$ for $N=200$ (runs 46–50) and for $N=400$ (runs 51–52). The results for $N=200$ and $N=400$ are in excellent agreement with each other and both agree fairly well with the experimental radial distribution function [2]. In particular, the so-called split maximum is observed in the simulations. Some deviation from the experiment, especially for large $r/a$, may be due to a limited number of particles in [2], since $N=8000$ may be insufficient for a physical system (which does not allow for periodic boundary conditions) to eliminate finite-size effects.

It is of special interest to compare our results with those obtained by the method [19], since the latter seems to be the only published *kinetics-dependent* packing algorithm for periodic boundary conditions which cannot lead to *complete* crystallization. The algorithm (see Section 1 and [19, 22] for detailed description) depends on $N$, "densification rate" $k=\tau^{-1}$, and the choice of initial uniform random distribution of points in a cube. For the limited use in the present work, a much simpler (but far less efficient) code, than in [19, 22, 23], was written, without a chaining mesh and linked-list structure. The calculations are presented in Fig. 4 for different initial distributions. The average packing densities

$$\langle c \rangle = 0.642 \pm 0.001 \qquad (N=\ 50,\ \tau=25000)$$
$$\langle c \rangle = 0.644 \pm 0.001 \qquad (N=\ 50,\ \tau=50000)$$
$$\langle c \rangle = 0.655 \pm 0.002 \qquad (N=100,\ \tau=50000)$$

imply that, to a good accuracy, the value 0.644 can be taken as a $(\tau \to \infty)$-limit for $N=50$ and 0.655 as a lower bound of this limit for $N=100$. The linear in $N^{-1}$ extrapolation of the values 0.644 and 0.655 suggests 0.666 as a *lower* estimate for the packing density of algorithm [19] in the limit $\tau, N \to \infty$. The latter value is consistent with the limited number of calculations for $N=200$, $\tau=10^5$ (see Fig. 4, the average being 0.664). A different limit 0.649–0.650 of the packing density for this algorithm was reported [19, 23], and some deviation from our calculations is not clearly understood. Anyway, compared to our algorithm (see Table II and

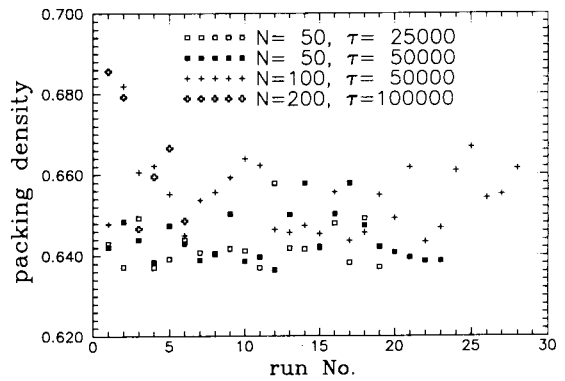


FIG. 4. The packing density for different irregular configurations of spheres prepared by Jodrey and Tory's method [19].

Fig. 1), the method [19] yields appreciably higher packing densities, which should be due to some crystallization for large $\tau$ (especially considering that the densities as high as 0.68 were observed for some realizations, see Fig. 4). In contrast, "rough" packings (with noticeable gaps between particles) prepared by method [19] with "not too large" values of $\tau$ can be considered as quite random. For instance, when a configuration generated by method [19] at $N=100$, $\tau=500$ (with $c=0.624$) was used as a starting state for our algorithm, the final density proved to be 0.632, close to the values presented in Fig. 1 for $N=100$. In different experiments, with much higher values of $\tau$, it was observed that a packing prepared by method [19] can be very slightly densified by our algorithm, but the final close-packed state contains some particles with less than three neighbors (and even free spheres). So, along with partial crystallization, the effect of algorithm [19] for large $\tau$ is likely to produce some "holes." *The principal feature of our algorithm is that any crystallization in the final state* (which was presumably avoided in our calculations) *may be due only to some order in the initial configuration*, whereas the densification procedure [19] (as well as "hard-sphere fluid" compression, either by molecular dynamics or Monte Carlo method) is partially crystallizing *itself*. The fast method [19] could be used to prepare initial states for our algorithm, thus reducing a total computation time. However, the appropriate choice of $\tau$ is not obvious and this idea was not exploited in our calculations.

The experimental packing density $0.6366 \pm 0.0005$ [1] is appreciably lower than the $(N, \tau \to \infty)$-limit for the algorithm [19] and slightly below the best Berriman's estimate 0.642–0.645 (based on some extrapolation of the radial distribution function from the "fluid region" $c<0.49$ to much higher densities) [15]. This provoked a discussion [15, 19] of whether a true maximum of random close packing density was achieved in the experiments [1] with steel balls, or some friction inhibited progress towards the densest possible packing. The calculations using our algorithm indicate, however, that the experimental value 0.637 need not be revised, at least, considerably.

## 4. CONCLUDING REMARKS

An isotropic *kinetics-independent* algorithm has been constructed for random close packing of equisized spheres with triply periodic boundaries. The algorithm results in a perfect contact network with the average coordination number six (for particle number $N \gg 1$) and a system of normal reactions between the spheres maintaining the structure and prohibiting further densification. Both the experimental packing density (about 0.637) and radial distribution function are well reproduced by our algorithm. The normal forces in the final state are a part of the algorithm and can be used to calculate small elastic particle deformations by Hertz theory.

A relatively long computation time, due to a large number of bond separations, is, probably, the only discouraging feature of our algorithm. A typical run took from hours for $N=100$ to several days for $N=200$ on PC AT ACRO 386 c/Weitek 3167. Each of the two variants for $N=400$ took even more than a month of calculations. However, we are not aware of any other published algorithm which would have demonstrated an *unambiguous* convergence to the experimental results on random close packing. Despite the computational cost, a lot of random close-packed configurations have been calculated (see Table II and Fig. 1) and they are available on the request from the author. The computed configurations can be used, in particular, in simulating the effective conductivity of granular media, both for rigid and for slightly deformable inclusions.

Finally, it seems feasible to develop a similar isotropic algorithm for close packing of spheres with the average coordination number four, which may resemble pouring *absolutely rough* particles into a large vessel without vibration.

## APPENDIX: PROOF OF THE LEMMA

Let $(y_1, y_2, \ldots, y_N)$ be a new coordinate system with the origin $\mathbf{P}^{(m+1)}$ and basis vectors $\mathbf{e}_k = \mathbf{P}^{(k)} - \mathbf{P}^{(m+1)}$ $(1 \leqslant k \leqslant m)$. All the points $\mathbf{P}^{(i)}$, except $\mathbf{P}^{(k)}$, satisfy the $k$th equation (8). Hence, the $k$th equation of the system (8) for $1 \leqslant k \leqslant m$ is equivalent to $y_k = 0$. Besides, the last equation (8) determines a $(m-1)$-dimensional hyperplane containing $\mathbf{P}^{(1)}, \ldots, \mathbf{P}^{(m)}$ and should be equivalent to $y_1 + \cdots + y_m = 1$. So, the transformation from $x_i$ to $y_i$ is of the form

$$\begin{aligned} a_{k1}x_1 + \cdots + a_{km}x_m - b_k \\ = \lambda_k y_k \qquad \text{for} \quad 1 \leqslant k \leqslant m, \\ a_{m+1,1}x_1 + \cdots + a_{m+1,m}x_m - b_{m+1} \\ = \lambda_{m+1}(1 - y_1 - \cdots - y_m) \end{aligned} \tag{A1}$$

with some non-zero constants $\lambda_1, \lambda_2, \ldots, \lambda_{m+1}$ (the equations for $\lambda_j$ can be written but are not required here). Minimizing the function (10), written in the new coordinates, we have for the extremal point $\mathbf{x}^* = (y_1^*, \ldots, y_m^*)$,

$$\lambda_i^2 y_i^* = \lambda_{m+1}^2 (1 - y_1^* - \cdots - y_m^*) \qquad (1 \leqslant i \leqslant m). \tag{A2}$$

The solution of (A2) yields

$$\begin{aligned} y_i^* &= \lambda_i^{-2} \lambda_{m+1}^2 D, \\ D &= \left[ 1 + \lambda_{m+1}^2 \sum_{k=1}^{m} \lambda_k^{-2} \right]^{-1}. \end{aligned} \tag{A3}$$

Hence, the residuals (11)

$$\varepsilon_i = \lambda_i^{-1}\lambda_{m+1}^2 D \quad \text{for} \quad 1 \leqslant i \leqslant m, \qquad \varepsilon_{m+1} \Rightarrow \lambda_{m+1} D. \tag{A4}$$

On the other hand, the residuals (9) take the form

$$\delta_i = \lambda_i \quad \text{for} \quad 1 \leqslant i \leqslant m+1. \tag{A5}$$

The proof of (12) is completed by multiplying (A4) and (A5).

The statement (12) of the lemma has a clear geometrical sense. Consider an $m$-dimensional simplex $T$ with vertices $\mathbf{P}^{(1)}, \ldots, \mathbf{P}^{(m+1)}$, i.e., the minimal convex set containing all $\mathbf{P}^{(k)}$ (see Fig. 5 for $m=2$). The coordinates $y_1, \ldots, y_m$ yield the canonic description [31] of the simplex interior

$$y_i > 0 \quad \text{for} \quad 1 \leqslant i \leqslant m \qquad y_1 + \cdots + y_m < 1. \tag{A6}$$

The function (10) can be written as

$$F(\mathbf{x}) = \mu_1 d_1^2 + \cdots + \mu_{m+1} d_{m+1}^2, \tag{A7}$$

where $d_k$ is the distance from $\mathbf{x}$ to the plane of the $(m-1)$-dimensional face opposite to $\mathbf{P}^{(k)}$ and $\mu_k$ are some positive constants. The minimum of (A7) is always attained *inside* the simplex since the extremal point (A3) satisfies (A6) (that is the reason for $\varepsilon_i$ and $\delta_i$ to be of the same sign). On the other hand, any internal point $\mathbf{x}$ of $T$ satisfies the constraint

$$S_1 d_1 + \cdots + S_{m+1} d_{m+1} = \text{const} = mV, \tag{A8}$$

where $S_i$ is the measure of the $(m-1)$-dimensional face opposite to $\mathbf{P}^{(i)}$ and $V$ is the total simplex volume (see Fig. 5 for $m=2$). Minimizing (A7) as a function of $d_1, \ldots, d_{m+1}$ under the constraint (A8) yields $\mu_i d_i / S_i = \text{const}$. On the other hand, $S_i = mV/H_i$, where $H_i$ is the distance from $\mathbf{P}^{(i)}$ to the opposite face plane. Hence,

$$\mu_1 d_1 H_1 = \cdots = \mu_{m+1} d_{m+1} H_{m+1} \tag{A9}$$

which is just another form of (12). These arguments generalize the elementary construction of the point inside a triangle with minimum $d_1^2 + d_2^2 + d_3^2$ [32]. This geometrical approach is, however, not quite rigorous (since the existence of the point $\mathbf{x} \in T$ satisfying (A9) should be proved), compared to the simple algebraic proof given above.

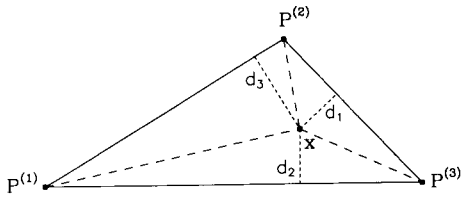


**FIG. 5.** Proof of the Lemma.

## ACKNOWLEDGMENTS

The author would like to thank Dr. M. Dekster (Bargiel), Professor E. M. Tory (Mount Allison University) and Professor J. D. Goddard (University of California, San Diego) for making available their works and helpful communications.

## REFERENCES

1. G. D. Scott and D. M. Kilgour, *Brit. J. Appl. Phys. Ser. 2* **2**, 863 (1969).
2. J. L. Finney, *Proc. R. Soc. London A* **319**, 479 (1970).
3. E. M. Tory, N. A. Cochrane, and S. R. Waddell, *Nature* **220**, 1023 (1968).
4. E. M. Tory, B. H. Church, M. K. Tam, and M. Ratner, *Can. J. Chem. Eng.* **51**, 484 (1973).
5. K. Gotoh, W. S. Jodrey, and E. M. Tory, *Powder Technol.* **20**, 233 (1978).
6. W. S. Jodrey and E. M. Tory, *Simulation* **32**, 1 (1979).
7. W. M. Visscher and M. Bolsterli, *Nature* **239**, 504 (1972).
8. M. J. Powell, *Powder Technol.* **25**, 45 (1980).
9. A. J. Matheson, *J. Phys. C* **7**, 2569 (1974).
10. C. H. Bennett, *J. Appl. Phys.* **43**, 2727 (1972).
11. D. J. Adams and A. J. Matheson, *J. Chem. Phys.* **56**, 1989 (1972).
12. W. S. Jodrey and E. M. Tory, *Powder Technol.* **30**, 111 (1981).
13. E. J. Le Fevre, *Nature Phys. Sci.* **235**, 20 (1972).
14. V. C. Aguilera-Navarro, M. Fortes, M. deLlano, and A. Plastino, *J. Chem. Phys.* **76**, 749 (1982).
15. J. G. Berryman, *Phys. Rev. A* **27**, 1053 (1983).
16. B. J. Alder and T. E. Wainwright, *J. Chem. Phys.* **33**, 1439 (1960).
17. L. V. Woodcock, *J. Chem. Soc., Faraday Trans. II* **72**, 1667 (1976).
18. C. A. Angell, J. H. R. Clarke, and L. V. Woodcock, *Adv. Chem. Phys.* **48**, 397 (1981).
19. W. S. Jodrey and E. M. Tory, *Phys. Rev. A* **32**, 2347 (1985).
20. G. K. Batchelor and R. W. O'Brien, *Proc. R. Soc. London A* **355**, 313 (1977).
21. A. Z. Zinchenko, *J. Comput. Phys.* **111**, 120 (1994).
22. M. Bargiel and J. Moscinski, *Comput. Phys. Commun.* **64**, 183 (1991).
23. J. Moscinski, M. Bargiel, Z. A. Rycerz, and P. W. M. Jacobs, *Mol. Simul.* **3**, 201 (1989).
24. N. A. Metropolis, A. W. Rosenbluth, M. N. Rosenbluth, A. N. Teller, and E. Teller, *J. Chem. Phys.* **21**, 1087 (1953).
25. L. D. Landau and E. M. Lifshitz, *Theory of Elasticity* (Pergamon, Elmsford, NY, 1959).
26. J. D. Goddard, X. Zhuang, and A. K. Didwania, in *Proceedings, 2nd Int. Conf. on Discrete Element Methods*, edited by J. R. Williams and G. G. W. Mustoe (ISEL Publ., MIT, MA, Cambridge, 1993).
27. R. W. Hockney and J. W. Eastwood, *Computer Simulation Using Particles* (McGraw-Hill, New York, 1981).
28. A. George and J. W.-H. Liu, *Computer Solution of Large Sparse Positive Definite Systems* (Prentice-Hall, Englewood Cliffs, NJ, 1981).
29. J. P. Hansen and I. R. McDonald, *Theory of Simple Liquids* (Academic Press, New York, 1976).
30. Y. M. Bashir and J. D. Goddard, *J. Rheol.* **35**, 849 (1991).
31. N. V. Efimov and E. R. Rosendorn, *Linear Algebra and Multidimensional Geometry* (Nauka, Moscow, 1974). [Russian]
32. D. O. Shklyarski, N. N. Chentsov, and I. M. Yaglom, *Geometric Inequalities and Extremal Problems* (Nauka, Moscow, 1970). [Russian]